

Non-imaging optical concentrators for low-cost optical interconnect

Robert P. Dahlgren*, Jacob A. Wysocki, Prof. Kenneth D. Pedrotti
Baskin School of Engineering, UC Santa Cruz
1156 High Street, Santa Cruz, CA 95064-1077 USA

ABSTRACT

In this work we report on a non-imaging optical concentrator for high-speed polymer optical fiber (POF), which has applications in chip-to-chip, consumer display, and backplane data transport. High-speed operation places demands on the ability of coupling from large-core media to small apertures typical of 10 Gbps optoelectronics. Design and fabrication of concentrators made by single point diamond turning and injection molding will be discussed, and comparison of experimental data to simulation will show good coupling efficiency with a wide tolerance to fiber misalignment.

Keywords: Non-imaging optics, optical data interconnect, fiber-optic modules, chip scale package

1. INTRODUCTION

In this work we investigate a non-imaging optical device that is well-suited for low-cost, high-speed optical interconnects that employ polymer optical fiber (POF) media. Low cost POF links having >10 Gigabit per second performance are desired for chip-to-chip, consumer display, backplane, and data communications applications^{1,2}.

A number of approaches have been tried for waveguide coupling, such as ball lenses, molded bi-convex lenses³, graded-index lenses⁴, and non-imaging concentrators employing reflection⁵ and total internal reflection⁶. Additional approaches include simple butt coupling⁷, aplanatic near-field optics⁸, Fresnel micro-optics⁹, photolithographic microlenses¹⁰, surface plasmon antennas¹¹, and diffractive optical elements¹². The concentrator proposed is a simple refractive aspheric that is amenable to standard package integration flow, and allows wide misalignment margins. Because of its small size, the insert can be molded at low costs from a material that is transparent at 850 nm such as polyetherimide (PEI).

2. METHODOLOGY

Chip-on-board (COB) packaging¹³ has been selected to provide a flexible platform during prototyping, and 50Ω controlled impedance striplines may be implemented with a 2-layer PCB. Beyond prototyping, COB was also selected because, as a package, it shares many characteristics with chip scale package (CSP) approaches¹⁴. Some CSP packages have low parasitic inductance and capacitance which is demanded for passing multi-gigabit/second (Gbps) data rates with high degree of signal integrity.

The CSP process achieves economies of scale by batch processing printed circuit board (PCB) panels containing many devices, using automated die pick & place, adhesive dispensing, wire bonding, and testing. Non-hermetic passivation is accomplished by overmolding of the PCB panels with a UL-rated epoxy using a transfer molding process, before the devices are separated into individual CSP packages.

2.1 Description of Collection Optics

Figure 1 shows the cross section of the device, called an optical insert, which contains the optical concentrator and a precision molded bore¹⁵. The insert is planar on one side, such that it may be more easily integrated into the COB

* rdahlgren@soe.ucsc.edu; phone +1.831.459.4283

assembly, being parallel to the substrate. The insert has many design features, such as ledge to limit the fiber insertion depth, a funnel to ease fiber insertion, fiducial markings, retention features, and gap-setting features (not shown).

The die-form optoelectronics (O/E), which can be a vertical cavity surface emitting laser (VCSEL) for a Tx or a photodetector for a Rx assembly, is mounted to the die attach pad with adhesive. The gap between the flat side of the insert and the substrate is filled with a UV-activated adhesive, which is cured when the optical insert is placed, permanently attaching the insert.

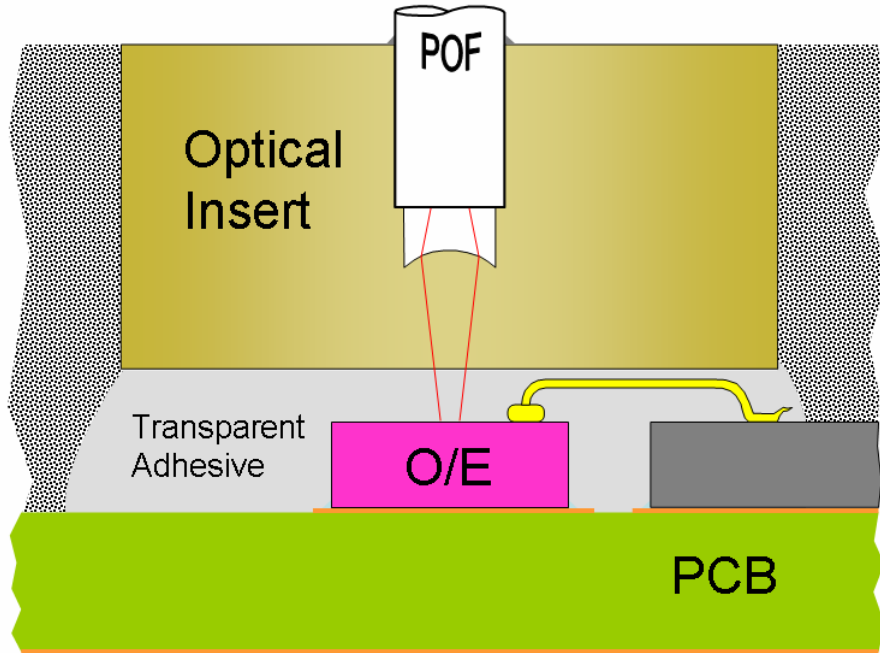


Figure 1. Cross-section of optical insert with optoelectronic die, wirebonding, and silicon die. The optical insert contains the alignment features for the fiber, an air gap, and the non-imaging optical concentrator.

The transparent adhesive serves a number of other purposes: it keeps contamination including the opaque epoxy out of the optical path, protects the delicate wirebonds, and provides a non-hermetic seal. For the prototypes “glob top” encapsulation compound would be applied at room temperature and pressure instead of hot transfer molding. The assembly is intended to provide an integrated fiber receptacle, collection optics, and electrical package that is simple to breadboard and manufacture.

2.2 Optical Design

After reviewing a number of imaging and non-imaging optical approaches, a refractive nonimaging approach was selected that does not require a reflective coating or a high aspect ratio structure. A filled backside gap was chosen such that the collection optics would have only one major refracting surface, and to the extent that refractive index could be matched, reduce parasitic reflections in the optical system.

Following the design methodology described elsewhere¹⁶, Table 1 summarizes the optical design for the transmitter configuration. The optical source in this case was modeled using 6 ~ 8 field points located on a 10 μm circle, each field point having an object space NA of 0.16 (the VCSEL divergence must be reduced by $\sim 1/n_{\text{adhesive}}$) and Gaussian apodization. This was done in an attempt to approximate the annular Laguerre-Gaussian and Hermite-Gaussian mode structure¹⁷ of multimode VCSELs, which changes dynamically with instantaneous forward bias current. The output aperture of the VCSEL is at the object plane, and the coordinate break at surface 1 will be used during subsequent Monte Carlo simulations, for statistical misalignment of the O/E with respect to the insert optical axis. Similarly, the two coordinate breaks at surfaces 5 and 6 will be used to apply misalignment between the optical axis and the optical fiber

endface, which is located at the image plane. The image plane has a fixed semi-diameter and constrained NA per the fiber manufacturer’s specifications, to define the acceptance cone of the fiber.

For a receiver topology the order would be reversed with the object being the fiber endface, with a suitably modified set of field points. The image plane would now contain the photodetector (which does not have a limited acceptance angle).

Table 1. Optical Design, units are in millimeters. Lens edge thickness was 0.375 millimeters.

Surf	Type	Comment	Radius	Thickness	Glass	Semi-Dia	Conic
OBJ	Standard	VCSEL	Infinity	0.0000		0.3750	0.0000
1	Coord. Break	Placement		0.0000	-		
2	Standard	Adhesive Gap	Infinity	0.2000	1.560	0.3750	0.0000
3	Standard	Back of Insert	Infinity	0.5000	1.630	0.3750	0.0000
STO	Standard	Concentrator	-0.195	0.6000	1.000	0.3000	-0.640
5	Coord. Break	Fiber Tilt		0.0000	-		
6	Coord. Break	Fiber Decenter		0.0000	-		
IMA	Standard	Fiber 120um	Infinity	-	1.350	0.0600	0.0000

It was attempted to design the system to have a short overall length, yet still be moldable, i.e. a minimum feature thickness is about 500 μm to avoid the “potato chip” effect. The adhesive gap is set to a value of 200 μm from the surface of the optoelectronics, to provide a minimum clearance for the bond wires. The UV-activated adhesive has a refractive index of 1.56 and is sufficiently transparent at 850 nm.

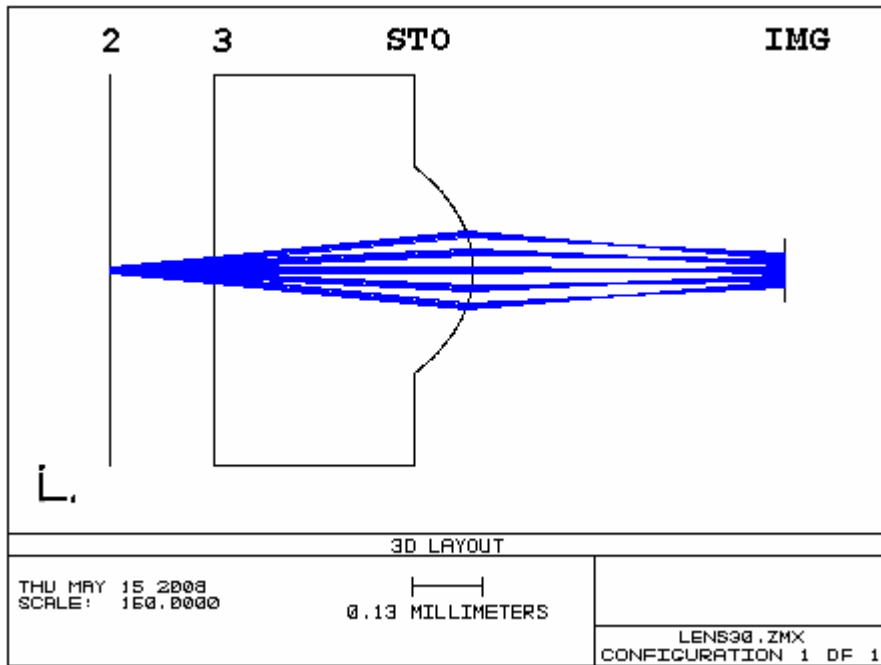


Figure 2. Layout of optical concentrator within the insert showing the object (coincident with surface 2). For the same reason the coordinate breaks are not visible in this layout but are coincident with the object and image planes.

The distance from the planar side of the insert to the vertex of the ellipsoid is 500 μm. The convex surface is the shape of an ellipsoid of rotation about the z-axis, described by Eq. (1) having a radius of R = 195 μm and a conic constant defined as K = -0.64 (per Kingslake). The parametric equation of the surface is given by

$$(1 + K)z^2 - 2zR + (x^2 + y^2) = 0 \tag{1}$$

With the x and y values limited by the surface’s clear aperture (stop) diameter of 400 μm.

The air gap between the vertex of the curved surface and the endface of the optical fiber is 600 μm deep, as shown on the right hand side of the layout in Figure 2. The PEI material has a refractive index of 1.633 at 850 nm wavelength, sufficiently matched to the gap adhesive to reduce Fresnel reflections at the planar surface.

2.3 Substrate Design

The prototype COB substrate is a PCB made of a dielectric material such as Rogers RC4003, replacing the standard tinning of the PCB pads with 30 microinches ($\sim 0.8 \mu\text{m}$) of soft gold plating over 150 microinches of nickel. The plating layers are optimized for wirebonding with 1 mil ($\sim 25 \mu\text{m}$) Au wire on a K&S wirebonder. Soldermask and silkscreen layers were not used on the prototype PCB because it would have modified the transmission line impedance; for a mass production substrate materials must be selected to tolerate the high temperature excursions during the transfer molding process during package integration and reflow soldering upon end use.

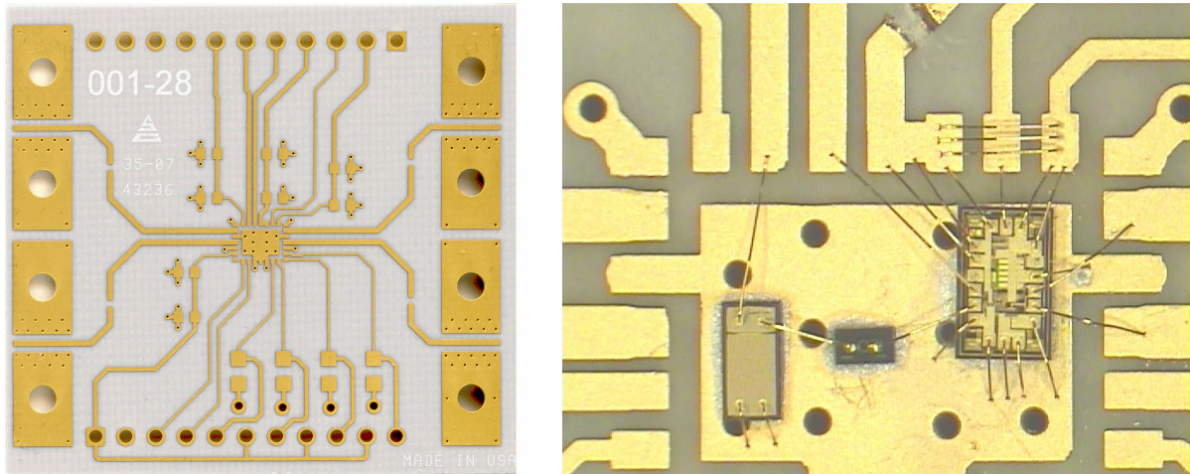


Figure 3. Photograph of 40 mm x 40 mm substrate for COB and magnified view die attach pad populated with commercial optoelectronic and electronic dice. The central die is a GaAs PIN photodiode, the left component is a 180 pF chip bypass capacitor, and the IC on the right is a commercially available transimpedance amplifier.

Three substrate board designs were made using standard CAD design tools, for transmitter testing and for receiver testing of commercial and custom electronics. High quality straddle-mount RF microstrip launchers¹⁸ were used to interface with lab instrumentation via semi-rigid 50 Ω cables. Power and other electrical connections were made through single-row headers.

2.4 Prototype Fabrication

Before a single-cavity mold was finalized, a set of prototypes concentrators without the POF alignment bores were generated by single-point diamond-turning. Starting with a 3 millimeter disc of PEI, the curved surface was diamond-turned onto the face of the disc, with surface figure irregularity specified less than 2 fringes p-v using a 550 nm double-pass interferometer ($\sim \pm 0.3 \mu\text{m}$ error). A photograph of the disc and a detail of the central curved surface is in Figure 4, careful examination reveals an annular undercut beyond the ellipsoidal surface, which is an artifact of the finite radius of the diamond tool.

According to Table 1, the planar side of the prototype insert must be brought into a very close proximity to the O/E and maintain position without damaging the bond wires, which demanded a very stiff mechanical design. Front and side observation at high magnification during the approach and alignment phases also prohibited traditional lens mounting methods. Therefore an arm made of tool steel with a 2 millimeter diameter aperture was fabricated, and subsequently hardened and thinned into a 250 μm thick blade as shown in Figure 5 (the large hole is for attachment to an XYZ linear translation stage). After careful deburring and inspection of the aperture, the non-optical portion of the prototype disc could be bonded to the blade with an appropriate adhesive or blocking compound.

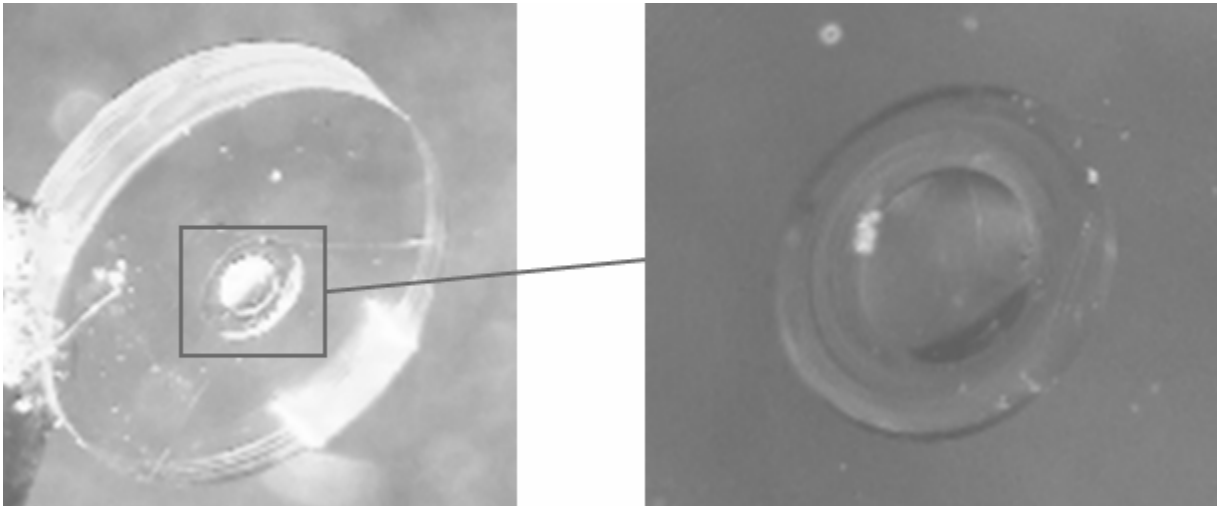


Figure 4. Photograph of diamond-turned polyetherimide (PEI) optical concentrator with detail of aspheric surface.



Figure 5. Photograph of blade and mounted diamond-turned prototype from planar side (L) and curved side (R).

2.5 Electronics Fabrication

For the Rx COB, the substrate is manually populated with surface mount components prior to cleaning, die attach, and wirebonding operations. The chip photodetector used is a Cosemi MXP7001 GaAs PIN photodiode (75 μm aperture with < 250 fF capacitance) selected for its wide bandwidth at low reverse bias voltage requirements. The photodiode die, commercial transimpedance amplifier die, and 180 pF chip bypass capacitor are mounted on the die attach pad with epoxy and cured for 30 minutes. Figure 3 shows a close-up of result after the wirebonding is accomplished for one Rx COB design.

After wirebonding and inspection the SMA microwave launchers and DC connectors are installed on the substrate, it is mounted in an aluminum frame to increase rigidity and provide a mechanical reference. The aluminum frame is designed to dovetail into the optical test setup for a repeatable, quickly swappable mechanical interface common to the various COB designs.

The Tx COB employs a commercial laser diode driver and a similar prototyping process as the Rx COB, with the complication that the very small VCSEL dice ($\sim 250 \mu\text{m}$ on each side) make manual placement challenging. The 850 nm VCSEL source is a Philips ULM850-10-TN-N0101U die that has one wirebonding pad for the anode and uses a backside contact for the cathode, which means that an electrically conductive die attach epoxy is necessary. All of the COB electronics and test instrumentation are very susceptible to ESD and physical damage so static and contamination control are critical during the assembly and testing process.

3. DATA

Test methods will be presented for the completed Tx and Rx COB assemblies. After a COB assembly passes continuity testing it is mounted in the optical setup such that the optical axis of the COB is parallel to the laboratory optical bench as in Figure 6, to reduce the possibility of contamination and facilitate viewing.

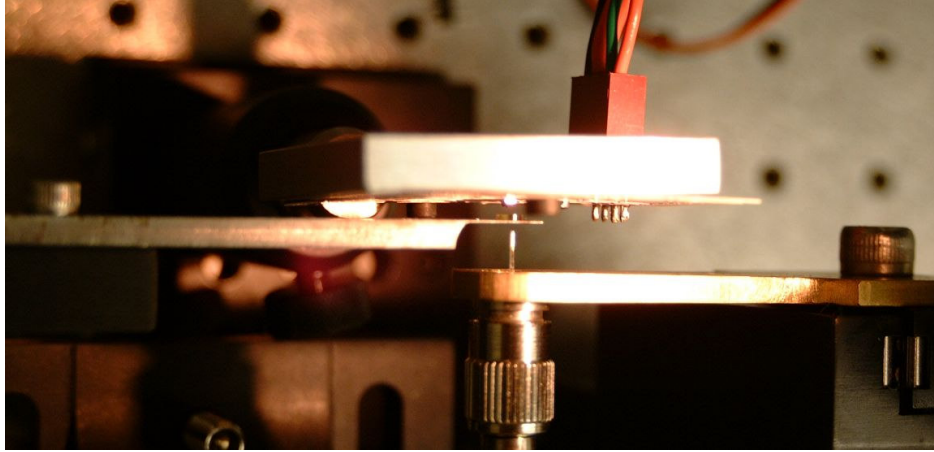


Figure 6. Top view of test setup for COB showing the edge of the PCB, the prototype collection optics and the POF.

A pair of XYZ translation stages support the lens holder and the POF without risk of damaging the delicate wire bonds. The COB is connected to its external support electronics power supply, bias circuit, and monitoring instrumentation, and the stereomicroscope is used to carefully bring the optical element and the POF endface into close proximity to the O/E die.

3.1 Experimental Setup for Rx

A block diagram of the high speed test setup for the Rx COB is shown in Figure 7. A 10 Gbps optical bitstream provided by a pulse pattern generator in conjunction with an 850 nm 'reference' electrical-to-optical converter (California Scientific V126) was used to evaluate the Rx COB prototypes.

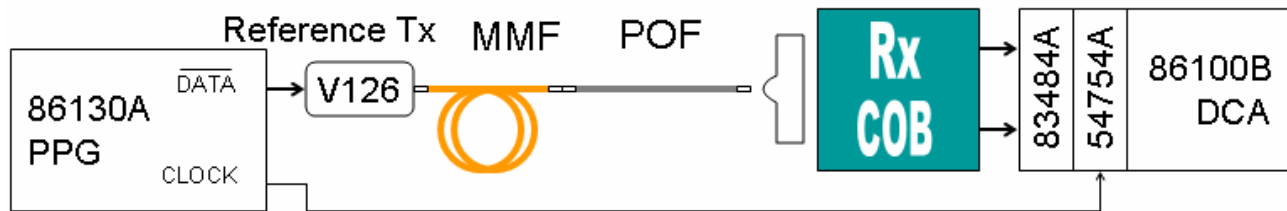


Figure 7. Block diagram of the COB receiver test setup. A pulse pattern generator (PPG) is the signal source and the digital communications analyzer (DCA) is used to characterize the Rx performance.

The reference transmitter had a 50/125 multimode fiber output so a 2 meter length of FC-connectorized glass multimode fiber was used to interface the reference transmitter to the POF sample, using an FC bare fiber adapter to mate the POF to the glass multimode fiber. The transmitter has a limited optical extinction ratio which was noted, and no efforts were made for any special launch conditioning or mode scrambling in the optical fibers. The Rx was tested with 0.3 meters of Chromis perfluorinated GigaPOF graded-index optical fiber having a core diameter of 120 μm .

3.2 COB Transmitter and Receiver

Once the COB receiver was tested, the Tx-Rx link was demonstrated by removing the reference transmitter and replacing it with the prototype Tx COB, as illustrated by the block diagram in Figure 8. For all testing, a pseudo random bit sequence of $2^{31}-1$ was used at a rate of 10 Gbps.

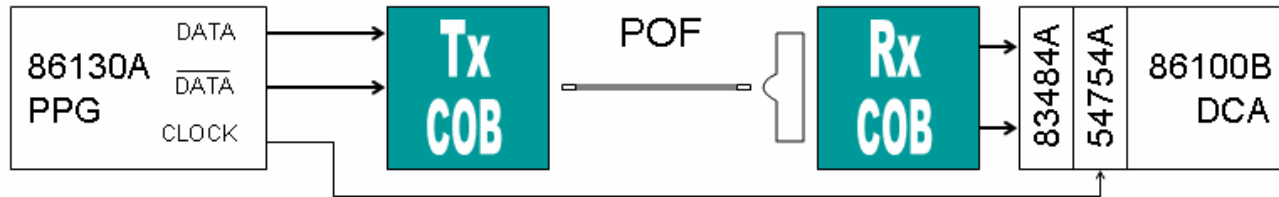


Figure 8. Block diagram of the COB transmitter and link test setup.

Optical butt coupling was used for the POF-to-VCSEL coupling on the Tx COB, and the optical concentrator was used on the Rx COB. Again, no special effort was made to condition the launch or mode scramble the POF. The digital communication analyzer acquires received bitstream for a length of time and displayed an eye pattern and the jitter, SNR, and other characteristics are computed and recorded.

4. RESULTS

Test results are presented for the completed Tx and Rx COB assemblies using the experimental setups described earlier.

4.1 COB Receiver

The Rx COB was evaluated in the setup described in Figure 7 with the reference transmitter at 10 Gbps. Figure 9 is an eye pattern for this example, showing good SNR and jitter characteristics after approximately 10^{15} bits were acquired.

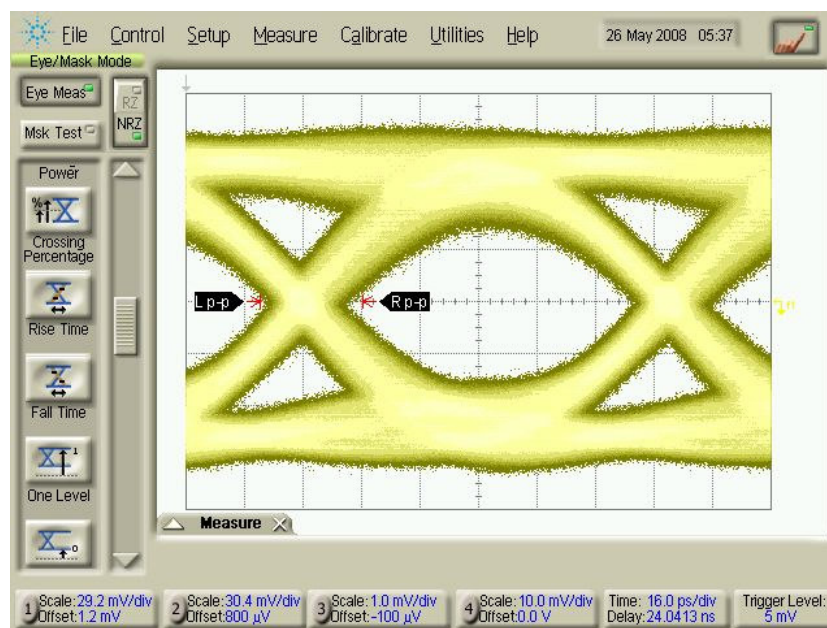


Figure 9. Eye diagram for Rx COB with reference transmitter operating at 10 Gbps for 30 hrs.

A symmetrical eye pattern was observed, and temporal histograms sampled at the eye crossing indicate that the jitter is dominated by random processes. Misalignment studies indicate a power penalty of 3 dB (but no errors) observed for a fiber decentering of $\pm 50 \mu\text{m}$ and $\sim \pm 400 \mu\text{m}$ for Z displacement error indicating an insensitivity to misalignment.

4.2 COB Transmitter and Receiver

The Tx COB and Rx COB were measured as a link in the setup described in Figure 8, unfortunately a 10 Gbps BERT was unavailable and BER had to be inferred from the eye pattern.

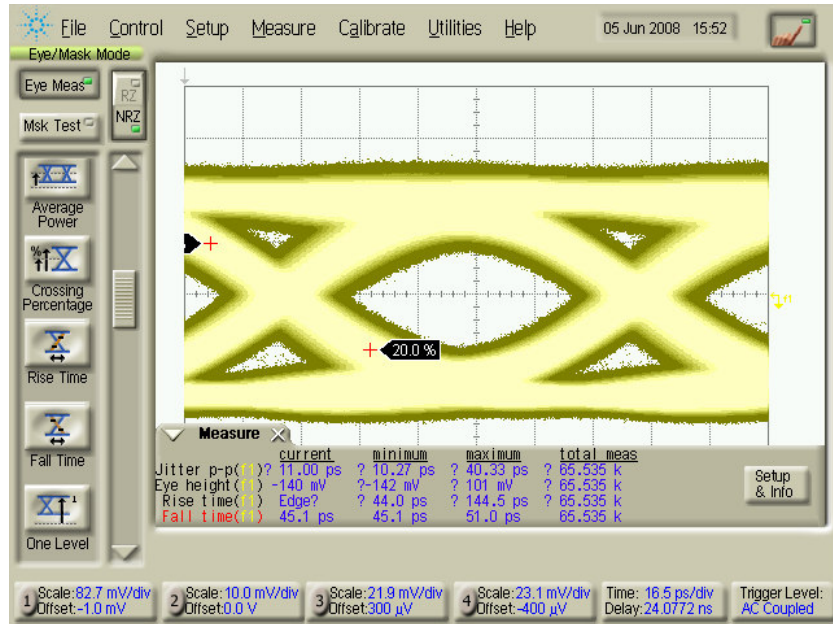


Figure 10. Eye diagram for 10 m POF link operating at 10 Gbps for 30 hrs.

After acquisition of approximately 10^{15} bits at 10 Gbps (30 hours) without observation of errors, it was possible to estimate the maximum bit error ratio with a high degree of confidence¹⁹.

Table 2. measured performance at 10 Gbps over 10 meters of POF

Estimated bit error ratio	$< 10^{-14} : 1$	CL = 99.99 %
Total jitter peak-to-peak	40.3	ps
Eye height	98.0	mV
Rise time	44	ps
Fall time	51	ps

Typical performance is shown in Table 2, with roughly $600 \mu\text{W}$ of optical power was measured exiting the optical fiber, having an unknown optical modulation amplitude.

5. CONCLUSIONS

5.1 Conclusions

An optical packaging concept has been demonstrated at the prototype level with a PEI nonimaging concentrator, with link operation at 10 Gbps having low inferred error rates. The packaging platform will permit straightforward migration to mass production volume as the volume scales from prototype development and CSP pilot manufacturing.

5.2 Insert Fabrication

Once a molding vendor was qualified, and all of their mechanical and optical tolerances and limitations were understood, the vendor was contracted for the tool and die work for a single-cavity mold to make the optical insert. Figure 11 shows a macro photograph of the first article from of the pilot run of optical inserts, showing the cylindrical insert, and the gate and sprue for the inflow of polymer to the cavity.

Careful examination of the side view image reveals the primary and secondary bores within the optical insert, which are distorted by the curved outside surface of the insert. Once the insert is evaluated and the design iterated if necessary, taking into account polymer shrinkage factors, this design will be ready for production when a multi-cavity mold would be commissioned.

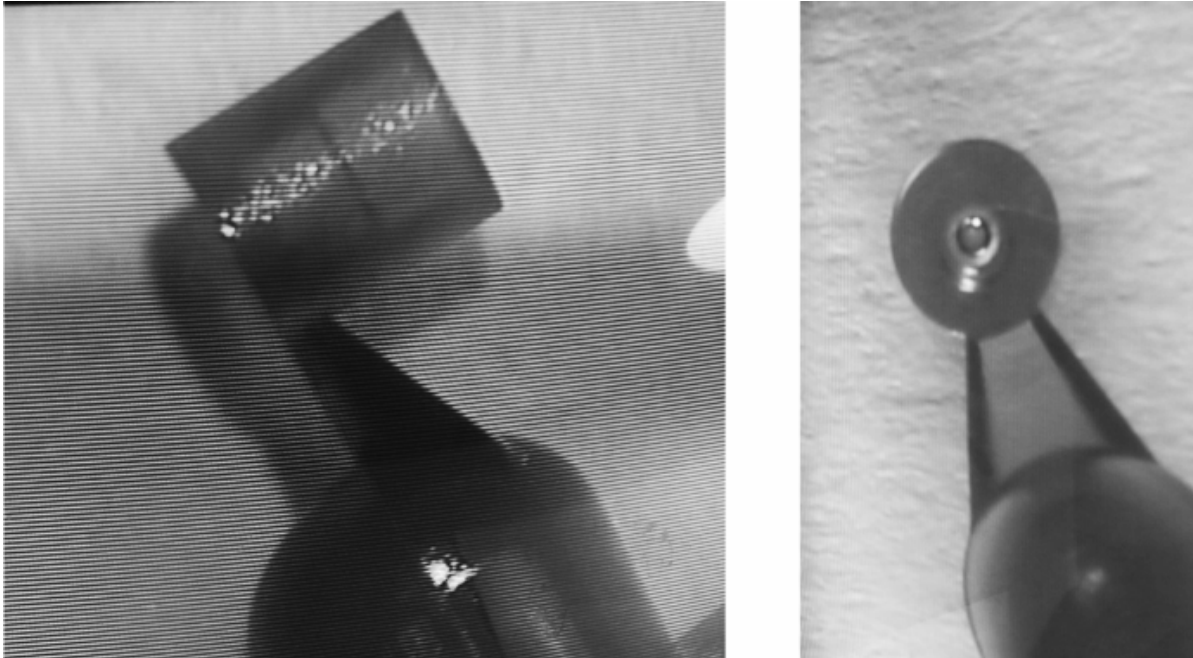


Figure 11. Side view (L) and front view (R) of optical insert as ejected from the single-cavity mold.

ACKNOWLEDGEMENT

The authors would like to acknowledge the support of National Semiconductor Corporation and the UC Discovery Grant program, Chromis Fiberoptics, and Qioptic Polymer, and Hamamatsu Corp. The technical contributions of Forest Martinez-McKinney at the Santa Cruz Institute for Particle Physics, and Stephen Peterson and J. M. Wincn at the UCSC Electrical Engineering Department, and Prof. Stephen Ralph at Georgia Institute of Technology is also gratefully acknowledged.

REFERENCES

- [1] Seager, M. K., "Requirements for high-speed interconnect for peta-scale simulation environments," POF World 16, Santa Clara, (2006).
- [2] Bennett, M. J., "The need for 100 Gig?," POF World 16, Santa Clara, (2006).
- [3] Heiney, A. J., Jiang, C. L. and Reysen, W. H., "Polymer molded lenses for optoelectronics," Proc. ECTC 45, 170-176 (1995).
- [4] Kuchta, D. M., et. al., "High speed data communication using 670nm vertical cavity surface emitting lasers and plastic optical fiber," Proc. ICPOF 3, 135-139 (1994).
- [5] Uehara, K., et. al., "High efficiency optical transceiver device for plastic optical fiber," POF World 12, Tokyo, 151-153 (2002).

- [6] Winston, R., et. al., [Nonimaging Optics], Elsevier, Oxford, (2005).
- [7] Ho, F., et. al., "Low cost transceiver components for short distance optical interconnects," Proc. ECTC 54, 1376-1380 (2004).
- [8] Nakar, D., Feuerman, D. and Gordon, J. M., "Aplanatic near-field optics for efficient light transfer," Optical Engineering 45(3), 1-8 (2006).
- [9] Rastani, K., et. al., "Integration of planar Fresnel microlenses with vertical-cavity surface-emitting laser arrays," Optics Letters 16(12), 919-921 (1991).
- [10] Strzelecka, E. M., et. al., "Monolithic integration of vertical-cavity laser diodes with refractive GaAs microlenses," Electronics Letters 31(9), 724-725 (1995).
- [11] Ishi, T., et. al., "Si nano-photodiode with a surface plasmon antenna," Japanese Journal of Applied Physics 44(12), 364-366 (2005).
- [12] Ghisoni, M., et. al., "Single and multimode VCSELs operating with continuous relief kinoform for focussed spot-array generation," IEEE Photonics Technology Letters 9(11), 1466-1468 (1997).
- [13] Lau, J.H., [Chip On Board: Technology for Multichip Modules], Van Nostrand Reinhold, New York, (1995).
- [14] For example National Semiconductor Corp. <http://www.national.com/packaging/parts/LAMINATECSP.html>
- [15] Dahlgren, R. and Pedrotti, K., "Tolerancing and corner cases in optical simulation," Proc. SPIE 7068, (2008).
- [16] Ibid.
- [17] Degen, C., Krauskopf, B., Jennemann, G., Fischer, I. and Elsäßer, W., "Polarization selective symmetry breaking in the near-fields of vertical cavity surface emitting lasers," J. Optics B: Quantum and Semiclassical Optics 2(4), 517-525 (2000).
- [18] Rosenberger model 32K243-40ME3 rated to 18 GHz used in conjunction with wideband 0.1 μ F capacitors for DC blocking (American Technical Ceramics 545L104KT).
- [19] Rudd, J., "Statistical confidence levels for estimating error probability," Maxim Engineering Journal 37, 12-15, (2000).